Theor Appl Climatol (2013) 111:471–481
DOI 10.1007/s00704-012-0677-z

ORIGINAL PAPER

A return to wet conditions over Africa: 1995–2010

Mark R. Jury

Received: 11 March 2012 / Accepted: 15 May 2012 / Published online: 1 June 2012

Abstract Climatic trends over sub-Saharan Africa are described using major river flows, European Community Medium-Range Weather Forecasts, Coupled Forecast System, global land surface data assimilation and National Center for Environmental Prediction reanalysis, Global Precipitation Climate Center gauge data, and satellite observations in the period 1995–2010. The Niger and Zambezi rivers reached flow levels last seen in the 1950s (2,000 and 5,000 m^3 s^{-1}, respectively), and rainfall across the Congo Basin increased steadily ~+0.16 mm day^{-1} $year^{-1}$. Weather events that contributed to flooding are studied and include the Zambezi tropical trough of 4 January 2008 and the Sahelian easterly wave of 19 July 2010. Diurnal summer rainfall increased threefold over the 1995–2010 period in conjunction with a strengthened land–sea temperature contrast, onshore flow, and afternoon uplift. 700 mb zonal winds over East Africa became easterly after 2001, so clean Indian Ocean air was entrained to the Congo, improving convective efficiency. Relationships between the African monsoon circulation and global teleconnections are explored. Zonal wind convergence around the Congo appears related with the tropical multi-decadal oscillation and signals in the Atlantic during the study period.

1 Introduction

The central African monsoon interacts with the regional circulation, and research has characterized its links with the Atlantic Ocean (Reason et al. 2006), the climate of northern and southern Africa (Hirst and Hastenrath 1983; Camberlin et al. 2001; Todd and Washington 2004; Jury et al. 2008), and intraseasonal pulsing (Mutai and Ward 2000; Tazalika and Jury 2008). Yet our understanding of its coupling with the global climate system is limited. Convection over central Africa is vigorous, and year-round lightning >50 km^{-2} is observed. But the convection is relatively inefficient due to aerosol loading (McCollum et al. 2000; Zipser 2003; Chen and delGenio 2008). Geerts and Tejene (2005) provide a satellite climatology of African convective structure, showing peak reflectivity near the 4-km level at 1500 hours local time. Seasonal north–south excursions of the intertropical convergence zone (ITCZ) are large over East Africa due to Indian monsoon winds (Hastenrath et al. 2011), swinging from the Zambezi Valley and Madagascar (10° S) in January to Ethiopia (10° N) in July. Further west, it tends to "pivot" near Gabon. The western segment of the African ITCZ oscillates from the Guinea coast into the Sahel (10° N) in August as the east Atlantic cold tongue develops. Rainfall reaches a maximum during October–November over the Congo when mean convective available potential energy exceeds 1,000 J kg^{-1}. At times, this air mass feeds into subtropical weather systems, as shown later.

With the advent of new reanalysis products that offer more realistic fields in the data-sparse tropics, it is useful to explore these to better understand African climate in the satellite era. The National Center for Environmental Prediction reanalysis (NCEP v2; Kanamitsu et al. 2002) offers six hourly ~180-km resolution fields since 1979, and the European Community Medium-Range Weather Forecasts (ECMWF, Dee et al. 2011) have an "interim" reanalysis product with a resolution of ~70 km. The National Aeronautics and Space Administration (NASA) undertakes a Modern-Era Retrospective Analysis for Research and Applications (MERRA) reanalysis that includes global land surface data assimilation (GLDAS) at 100-km resolution (Bosilovich 2008; Rienecker et al. 2011).

M. R. Jury (✉)
University of Zululand,
KwaDlangezwa, South Africa 3886
e-mail: mark.jury@upr.edu

M. R. Jury
Physics Department, University of Puerto Rico Mayagüez,
Mayaguez PR 00681, Puerto Rico

A 100-year ensemble reanalysis is available (Compo et al. 2006, 2011), and since 2009, NCEP has a reanalysis using the 64-layer Coupled Forecast System (CFS) at ~30-km resolution (Saha et al. 2010), similar to a regional version described in Mesinger et al. (2006). Bengtsson et al. (2007) and Anderson et al. (2009) have reviewed reanalysis data assimilation techniques and reliability; a useful summary is provided in Table 2.2 of Blunden et al. (2011). The CFS uses the Global Forecast System atmospheric model coupled with the ocean, assimilation of satellite radiances, surface-observed wind and precipitation via the NOAH model (Ek et al. 2003), surface temperatures underpinned by satellite infrared data (Smith et al. 2008), improved convective parameterization (Pan and Wu 1995; Hong and Pan 1996), and observed greenhouse gas concentrations. CFS also provides estimates of hourly rainfall.

This work is motivated by the change in African climate from a drying trend in the twentieth century (Hoerling et al. 2006) to frequent flooding in the early twenty-first century (http://wn.com/Africa_floods). Since the prolonged El Niño of 1995, river flows across Africa have increased (Amogu et al. 2010), and floods have displaced thousands of people (Jury 2010a, b). Processes underlying the return to wet conditions are sought, and the structure of two flood events is analyzed. The scientific questions to be addressed include: (1) Where has African rainfall increased fastest in the period 1995–2010? (2) What weather systems are responsible for floods across the Sahel and Zambezi? (3) Is there a regional circulation pattern associated with the return to wet conditions? (4) Has the amplitude of the diurnal cycle changed? (5) What external climate signals are involved? In Section 2, the data and methods are outlined. Section 3 provides evidence for a return to wet conditions in the period 1995–2010, analysis of flood weather over the Sahel and Zambezi, and a study of flood drivers at diurnal and interannual time scales, while conclusions are given in Section 4.

2 Data and methods

To understand the nature of hydrological fluctuations in the period 1995–2010, monthly river discharge records for the Niger River at Niamey (13° N, 2° E; 200 m elevation), the Congo River at Brazzaville (4° S, 15° E; 270 m), and the Zambezi River at Victoria Falls (18° S, 26° E; 930 m) are considered. These were drawn from the River Discharge database (Vorosmarty et al. 1998) via the IRI Climate Library, supplemented by recent records directly from the local river authority. Monthly rainfall fields are drawn from ECMWF-interim and CFS reanalysis, and Global Precipitation Climate Center v5 gauge analysis (GPCC; Rudolph et al. 2010) over sub-Saharan Africa (20° N–35° S, 10° W–50° E). Linear trends are analyzed via regression of 12-month smoothed anomalies per grid point for ECMWF rainfall, CFS rainfall, GPCC rainfall, CFS surface air temperature, and CFS 700-mb zonal wind. While a detailed discussion of the reliability of the various datasets is beyond the scope of this paper, an intercomparison of seasonal rainfall over the Congo area indicates agreement. All obtain a bimodal structure with an annual mean of 5.7 mm day^{-1} for ECMWF, 5.6 for CFS, and 4.1 for GPCC, compared with commonly used satellite merged products: (5.8) TRMM, (4.5) GPCP and CMAP (4.5) and (4.3) CAMS. Differences are minimized by analysis of anomalies and consideration of a 16-year period with consistent data assimilation. Intercomparisons are made with GLDAS and CFS estimated runoff and NASA satellite-observed vegetation (normalized difference vegetation index, NDVI, Leptoukh et al. 2007) anomalies averaged over the three rivers: Niger, 10–18° N,10° W–5° E; Congo, 10° S–6° N, 14–28° E; and Zambezi, 10–20° S, 20–27° E (cf. Fig. 2a). The runoff estimation is from a hydrological submodel within the GLDAS and CFS reanalyses, which depends primarily on rain rate and secondarily on evapotranspiration, soil characteristics, terrain slope, infiltration, and other factors.

Flood events for the Sahel (19 July 2010) and Zambezi (4 January 2008) are analyzed using daily rainfall from the Famine Early Warning System (FEWS; Love et al. 2004), NASA Cloudsat reflectivity, and NCEP v2 winds. To understand the diurnal contribution to flood trends, the hourly averaged rainfall for January each year is calculated from CFS data over the Zambezi (10–20° S, 20–27° E). Day–night differences over tropical southern Africa for January 2008 are analyzed using NCEP 850-mb air temperature, 700-mb winds, and 400-mb vertical motion. To describe the interaction of convection and aerosols over Africa, monthly NASA Total Ozone Mapping Spectrometer (TOMS) and Moderate-Resolution Imaging Spectrometer (MODIS) satellite aerosol optical depth (AOD) data are obtained, the latter offset and variance adjusted to match the former, and compared with the Congo area CFS rain rate divided by precipitable water (efficiency). Indices of CFS 12-month smoothed anomalies of Congo rainfall and Indian–East Africa (7° S–7° N, 25–50° E) and Gulf of Guinea (7° S–5° N, 10° W–20° E) 700-mb zonal wind are cross-correlated with global climate indices drawn from the Climate Explorer website. Values of $r > |0.40|$ are considered significant at 90 % confidence with 16 degrees of freedom.

3 Results

3.1 Evidence for a return to wet conditions

The monthly discharge of three major African rivers is given in Fig. 1a–c. The monthly flow of the Niger River at Niamey rises above 1,000 m^3 s^{-1} after July each year and has an upward

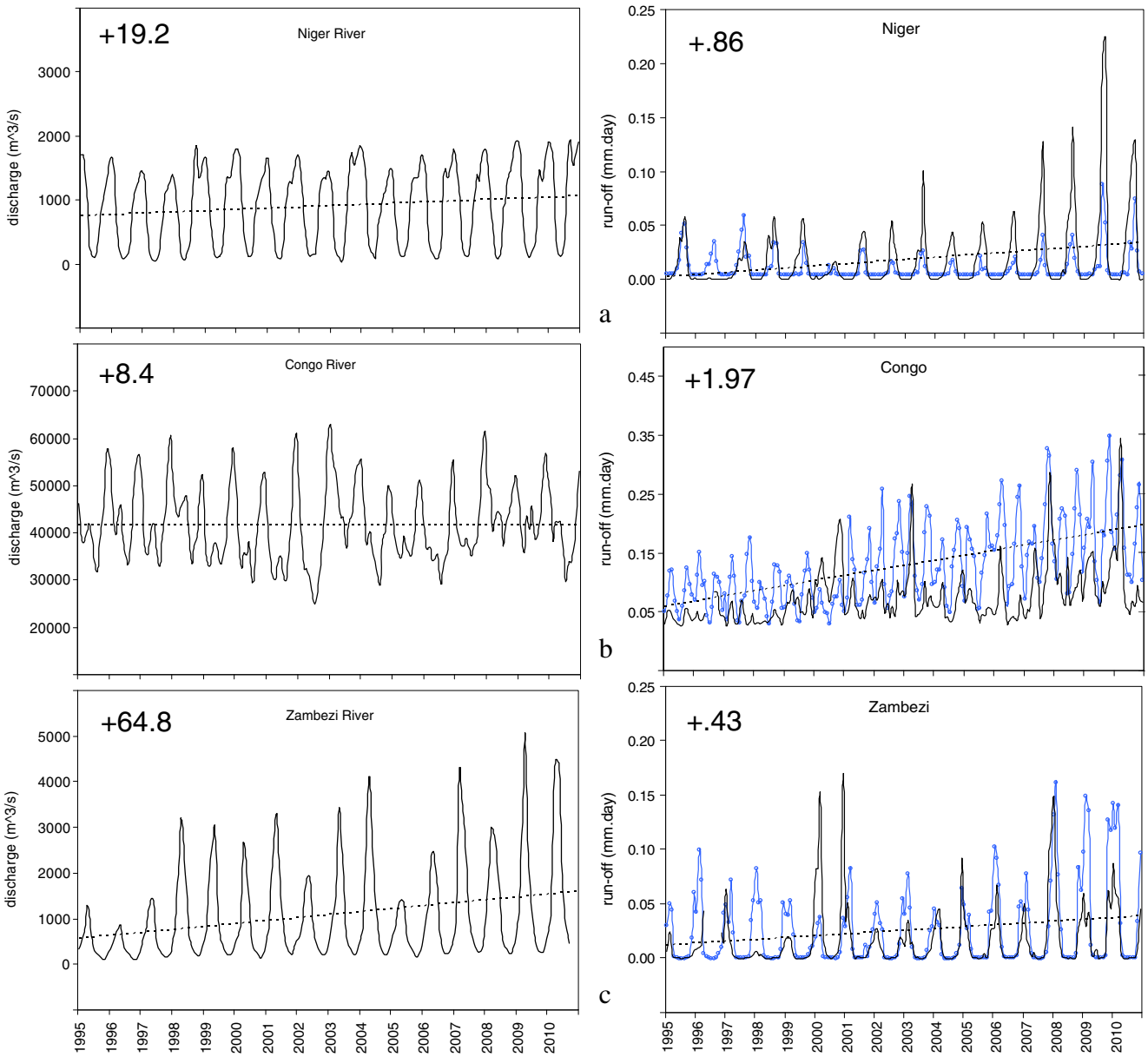

Fig. 1 Monthly observed discharge (*left*) and estimated runoff from GLDAS (*black*) and CFS (*blue*) for the **a** Niger River, **b** Congo River, and **c** Zambezi River, with linear trends (in cubic meters per second per year, *left*, and millimeters per year, *right*). Gauges and areas in Fig. 2a

trend of +19.2 $m^3\ s^{-1}\ year^{-1}$ in the period 1995–2010. In August 2010, its flow reached 2,000 $m^3\ s^{-1}$ for the first time since records began in 1929. Its subtropical catchment is 2.1×10^6 km^2, compared with 3.6×10^6 km^2 for the equatorial Congo River. The Congo discharge at Brazzaville averages $4.1\times10^4\ m^3\ s^{-1}$. Although it exhibits minimal trend since 1995 (+8.4 $m^3 s^{-1}\ year^{-1}$), Conway et al. (2009) found a significant up trend since 1979 (+103 $m^3\ s^{-1}\ year^{-1}$). The Zambezi River catchment covers 1.4×10^6 km^2 of the southern tropical highlands. Its flow rate at Victoria Falls exhibits an annual peak ~2,000 $m^3\ s^{-1}$ and a linear trend of +64.8 $m^3\ s^{-1}\ year^{-1}$ in the period 1995–2010. In 2009, it reached 5,000 $m^3\ s^{-1}$ for the first time since the 1950s. Monthly GLDAS and CFS estimated runoff averaged over the river basins is consistent with the flow trends, being upward in the Niger (+0.86 mm $year^{-1}$) and Congo (+1.97) and to less extent in the Zambezi (+0.43). These may seem like small numbers until the area (>10^6 km^2) is considered. Thus, hydrological trends in different climatic zones of Africa are upward since 1995, consistent with Olsson et al. (2005).

The trend in rainfall anomalies exceeds +0.2 mm $day^{-1}\ year^{-1}$ across the central African lowlands and Congo Basin 10° S–6° N in CFS reanalysis (Fig. 2a). ECMWF not only has up trends in parts of central Africa, but also shows down trends in the Sahel and Mozambique (Fig. 2b). Rainfall trends in the Congo Basin are higher for CFS

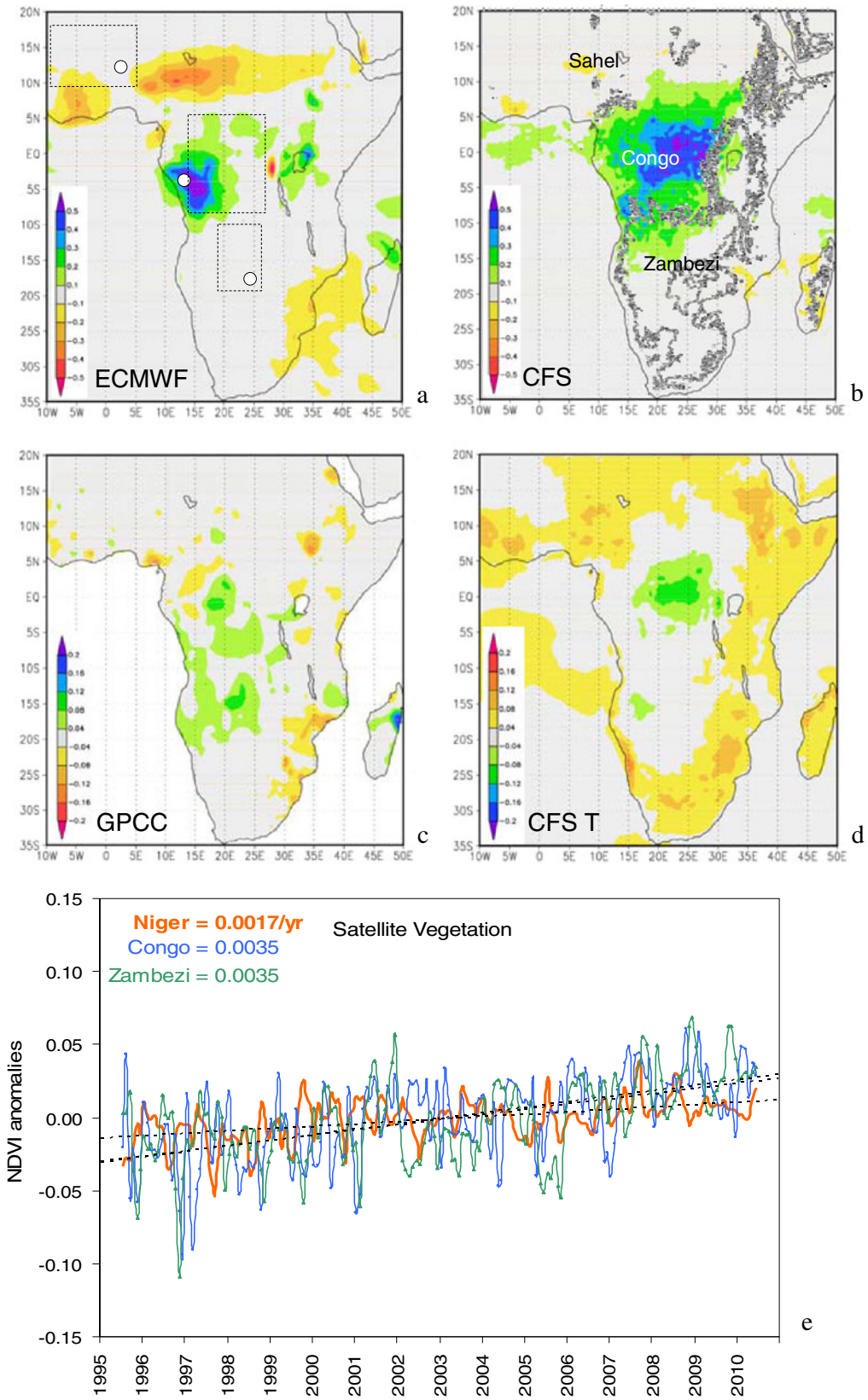

Fig. 2 Linear regression trends for smoothed monthly rainfall anomalies **a**ECMWF; **b** CFS; **c** GPCC gauge, all shaded *blue* = positive (in millimeters per day per year); **d** linear regression trends for CFS surface air temperature anomalies, *red* = positive (in degrees Celsius per year). River gauges and key areas are given in **a**, 1,000-m contour and key names in **b**. **e** Satellite vegetation anomalies in key areas, with trends

(+0.3 mm day^{-1} year^{-1}) than ECMWF (+0.06 mm day^{-1} year^{-1}) and GPCC (+0.03 mm day^{-1} year^{-1}) for reasons unknown. GPCC gauge rainfall anomaly trends are upward (+0.1 mm day^{-1} year^{-1}) over the Zambezi Valley (Fig. 2c) and downward over subtropical zones of East Africa (cf. Dinku et al. 2008). Hence, the return to wet conditions appears concentrated over central Africa, coincidently where station data are sparse. Surface air temperature anomalies exhibit the expected warming trend over the coastal plains (Fig. 2d, +0.15 C year^{-1}), while the Congo basin shows cooling in the period 1995–2010 according to CFS reanalysis. Changes in the thermal field can have secondary effects on the circulation. The $\partial T/\partial x$ gradient on the coast of East Africa (0° S, 40° E) could draw air from the Indian Ocean. The $\partial T/\partial y$ gradient north of the Congo (10° N, 15–30° E) could boost the African Easterly Jet and vorticity available to transient easterly waves.

Trends in satellite-observed vegetation (NDVI) anomalies averaged in each river basin are investigated (Fig. 2e). The Niger basin has the lowest mean vegetation fraction (0.27), and anomalies have a linear up trend of +0.017 year^{-1}, while the Congo and Zambezi basins, in closer proximity, have higher mean vegetation fraction (0.64 and 0.52, respectively) and trend upward at +0.035 year^{-1}. All have similar r^2 trend fit (~0.30) indicating consistent interannual variance. Thus, an objective measure of Africa's land surface confirms a return to wet conditions in the 16-year study period.

The intraseasonal behavior of African rainfall is analyzed by Hovmoller plot on 23° E using unfiltered CFS monthly anomalies (Fig. 3). Dry conditions prevailed from 1995 to 2000. There were isolated wet spells in austral summer in the south associated with El Niño/La Niña Southern Oscillation (ENSO) in 1998–1999. Rain anomalies became positive over the Congo after 2001 and strengthened in 2003 according to CFS. This can be traced to enhanced meridional moisture convergence near the ITCZ. In subtropical latitudes (Zambezi/Sahel), negative anomalies weakened by 2005. In 2006, positive rainfall anomalies spread from the Zambezi across the Congo into the Sahel by 2007. Thereafter, positive rain anomalies prevailed across Africa up to 2010. From this analysis, two cases are identified for further study.

3.2 Sahel floods

Up trends in river flow, runoff, and vegetation cover have been noted over the Sahel. These may be partly related to a strengthening of the southern Hadley circulation that feeds Congo air into seasonal weather systems. The African Easterly Jet accelerated >1 m s^{-1} after 2001 due to the aforementioned $\partial T/\partial y$, favoring more intense and frequent easterly waves. A case study flood event is analyzed for 19 July 2010 in Fig. 4a. Low-level flow from the Congo was drawn into the back of an easterly wave vortex at 14° N, 16°

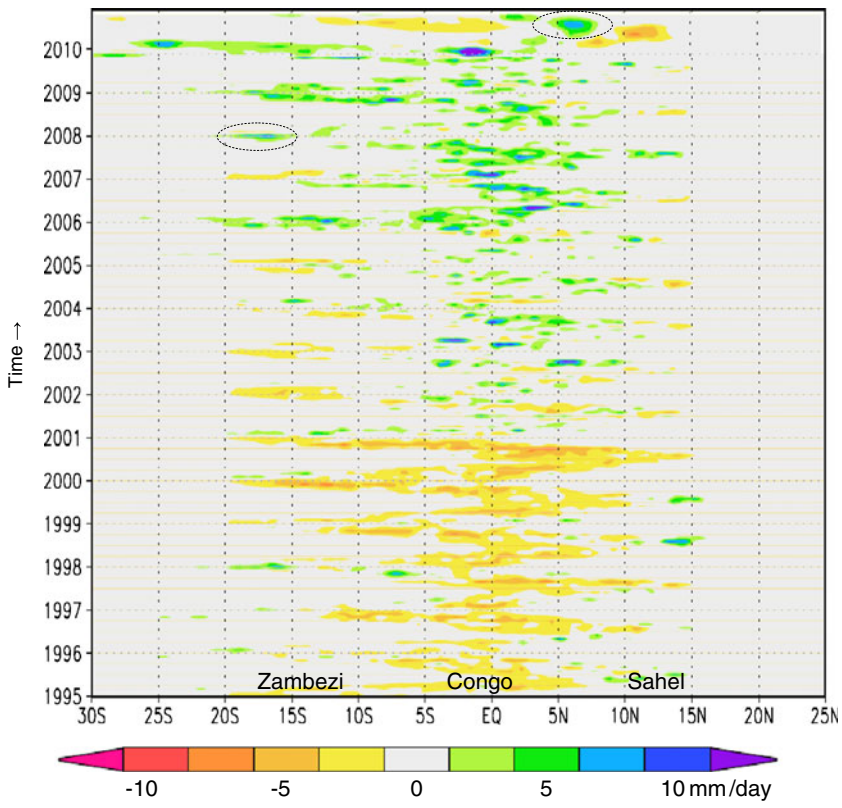

Fig. 3 Hovmoller plot on 23° E of monthly CFS rainfall anomalies. Case studies are *circled*

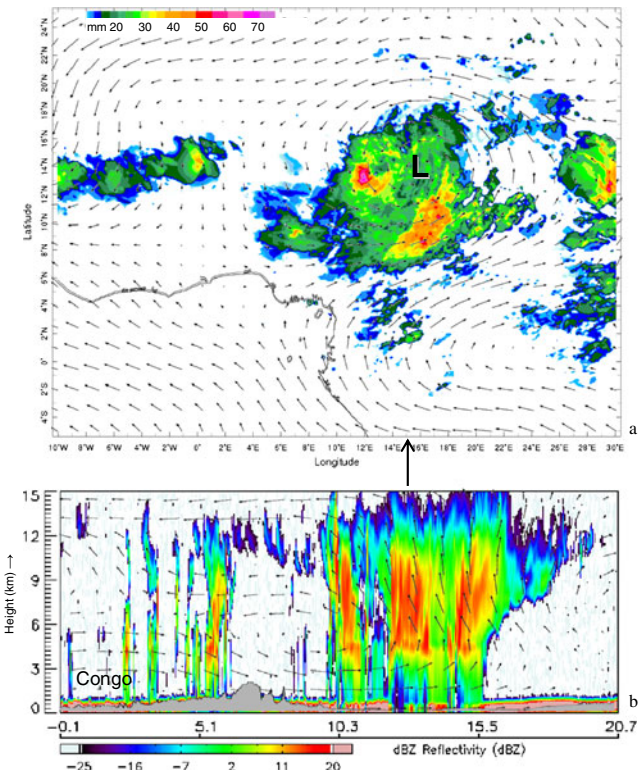

Fig. 4 **a** 19 July 2010 daily FEWS rain and NCEP 850- to 700-mb wind. **b** Cloudsat slice of reflectivity on 15° E at 13Z and NCEP VW wind. Largest vector=10 m s^{-1}; vertical motion exaggerated 30-fold

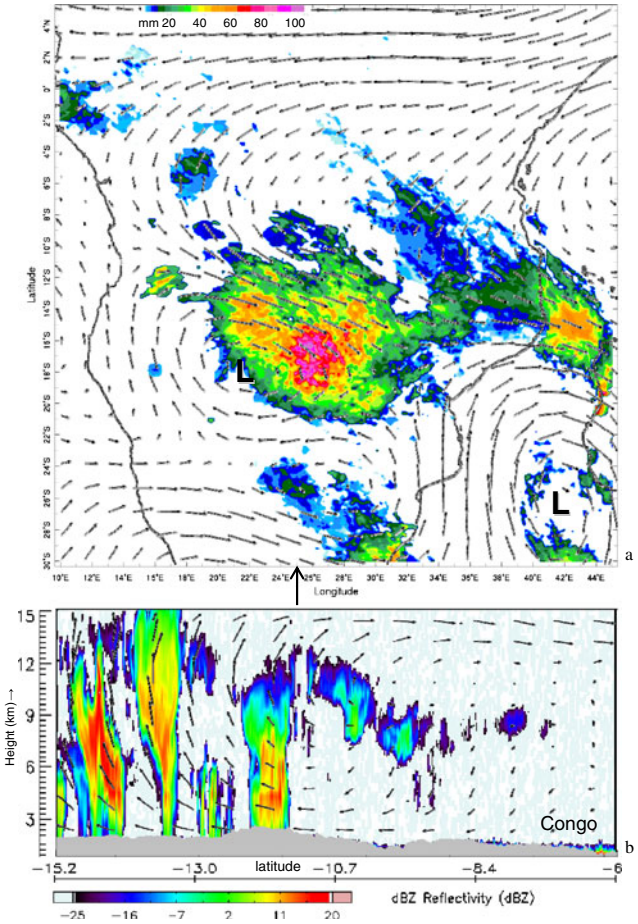

Fig. 5 **a** 4 January 2008 daily FEWS rain and NCEP 700-mb wind. Cloudsat slice of reflectivity on 25° E at 23Z and NCEP VW wind. Largest vector=10 m s^{-1}; vertical motion exaggerated 30-fold

E, as convection flared to the west. In the Cloudsat slice on 15° E at 13Z 19 July 2010 (Fig. 4b), highest reflectivity was observed in three towers from 10 to 15° N in the 4- to 10-km layer. The NCEP winds reveal a meridional overturning circulation with a center point at 8° N/5 km, connecting the Congo and Sahel. In that area, CAPE exhibited large diurnal oscillations (200–2,000 J kg^{-1}). Rain rates exceeded 50 mm day^{-1} over the Niger River valley as the wave progressed from 25° E to 10° W in 5 days (c=−8 m s^{-1}). The gaps between thunderstorm clusters were small, and successive easterly waves of 2,000-km wavelength were interconnected by cloud bands, so dry spells were limited. MODIS land surface temperatures in the zone 11–17° N were 4–8 °C below climatology in July–September 2010. Thus, lower evaporation contributed to soil saturation and flooding.

3.3 Zambezi floods

A case study flood event over the Zambezi Valley on 4 January 2008 is analyzed (Fig. 5a). A vortex had developed, similar to the Sahel case, and airflow was entrained from the Indian NE monsoon and equatorial Africa. Heavy rains were located on the east flank of a tropical trough. The Cloudsat slice on 25° E at 23Z 4 January 2008 and corresponding NCEP winds (Fig. 5b) show three main convective towers from 11 to 15° S with highest reflectivity in the southern tower from 3 to 9 km, where uplift was vigorous. The northern Hadley circulation provided a conveyor of low-level inflow from the Congo. The Zambezi troughs often link with the subtropical jet stream, evident here in a secondary low pressure at 27° S, 42° E (Fig. 5a).

A scientific question is whether the return to wet conditions is related to the diurnal cycle. The cumulative hourly averaged CFS January rain over the Zambezi area is plotted in Fig. 6a. Low diurnal amplitude was maintained in the period 2000–2004: a.m. and p.m. mean values were 1.9 and 3.7 mm h^{-1}, respectively. In the 2005–2009 interval, a.m. and p.m. values were 6.0 and 13.4 mm h^{-1}. Although the morning-to-afternoon ratio stayed near 2, there was a factor of 3 increase. The diurnal climate is analyzed in Fig. 6b–d by subtraction of 21–9Z night from 9–21Z daytime NCEP fields in January 2008. Daytime air temperatures in the boundary layer warmed 3 °C over East Africa and 4 °C over the Kalahari. Consistent with the land–sea temperature

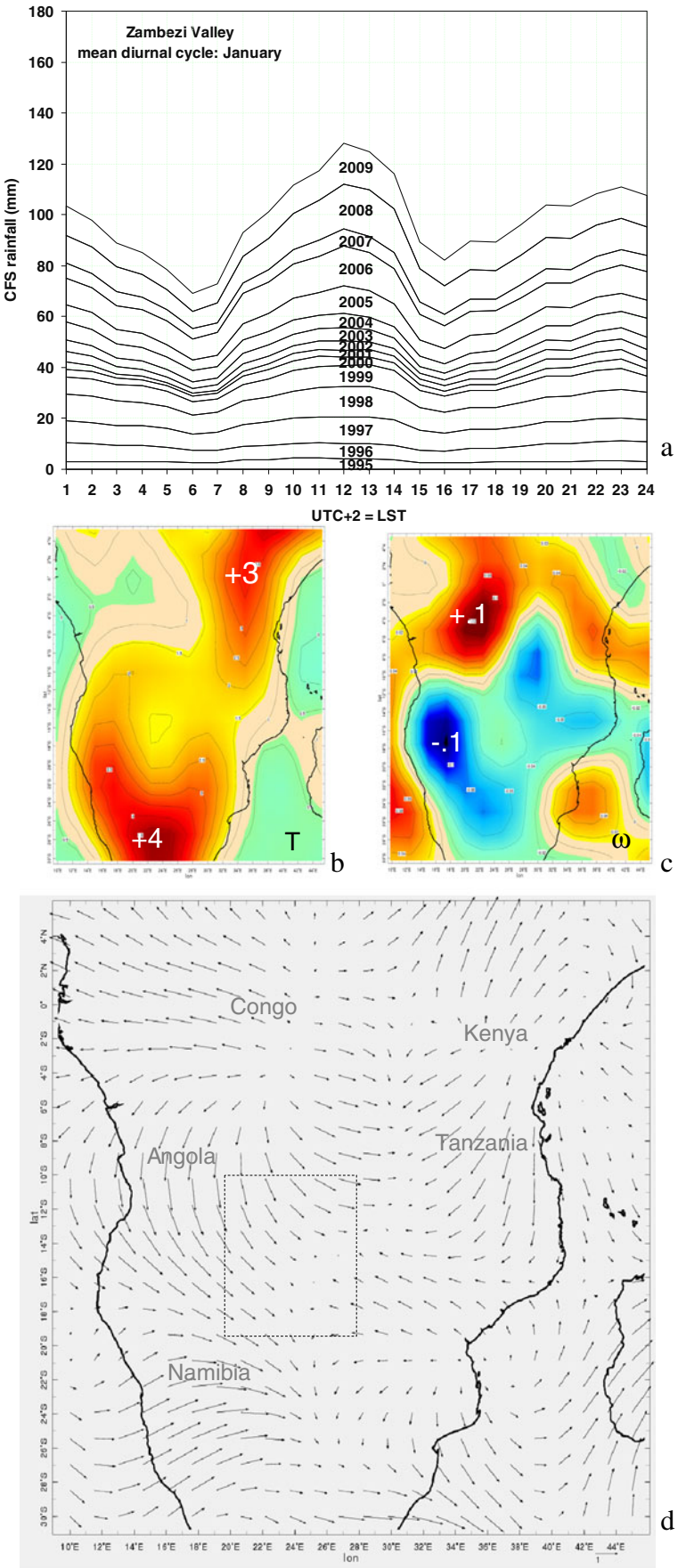

Fig. 6 **a** Cumulative diurnal amplitude of CFS January hourly rain over the Zambezi Valley (*box* in **d**). Mean day minus night differences of NCEP: **b** 850-mb air temperature, **c** 400-mb vertical motion (in pascals per second), and **d** 700-mb wind (largest=4 m s^{-1}), in January 2008

contrast, large-scale onshore flow developed with wind differences 2–3 m s^{-1} in the 700-mb layer over Tanzania, Angola, and Namibia (Fig. 6d). An unexpected feature was divergence over the Congo Basin and Kenya where subsiding motions were present in the 400-mb layer (Fig. 6c). The sinking air clears convection from equatorial Africa and feeds it toward the Zambezi during the daytime, creating two NW–SE axes of rising motion differences over the Kalahari and Rift Valley. So, flood trends are partially driven by afternoon thunderstorms and continental inflow, yet regional forcing may be important as explored below.

3.4 Factors contributing to wet conditions

The marked shift in rainfall over central Africa in 2001 (cf. Fig. 3) coincides with an increase of 700-mb easterlies from the tropical Indian Ocean, evident in the regression map (Fig. 7a). An area of negative values extends from the west Indian Ocean over the Rift Valley and surrounds the Congo Basin. The Indian–East African (IEA) wind anomaly time series (Fig. 7b) exhibits large positive (westerly) oscillations until 2001, whereafter it declines steadily to an easterly wind. The IEA index is significantly correlated with Congo rainfall (r=−0.85) and the Atlantic Multi-Decadal Oscillation (AMO, r=−0.43) in the period 1995–2010. The IEA index correlation with the Indian Ocean dipole mode (r=−0.30) and Pacific ENSO variables is weak. On the other hand, 700-mb zonal wind anomalies in the Gulf of Guinea are related to the North Atlantic Oscillation (NAO, r=−0.43) and to less extent Congo rainfall (r=+0.37). These Atlantic signals are part of the tropical multi-decadal circulation that affects Africa and South America (Ward 1998; Jury 2003; Bell and Chelliah 2006).

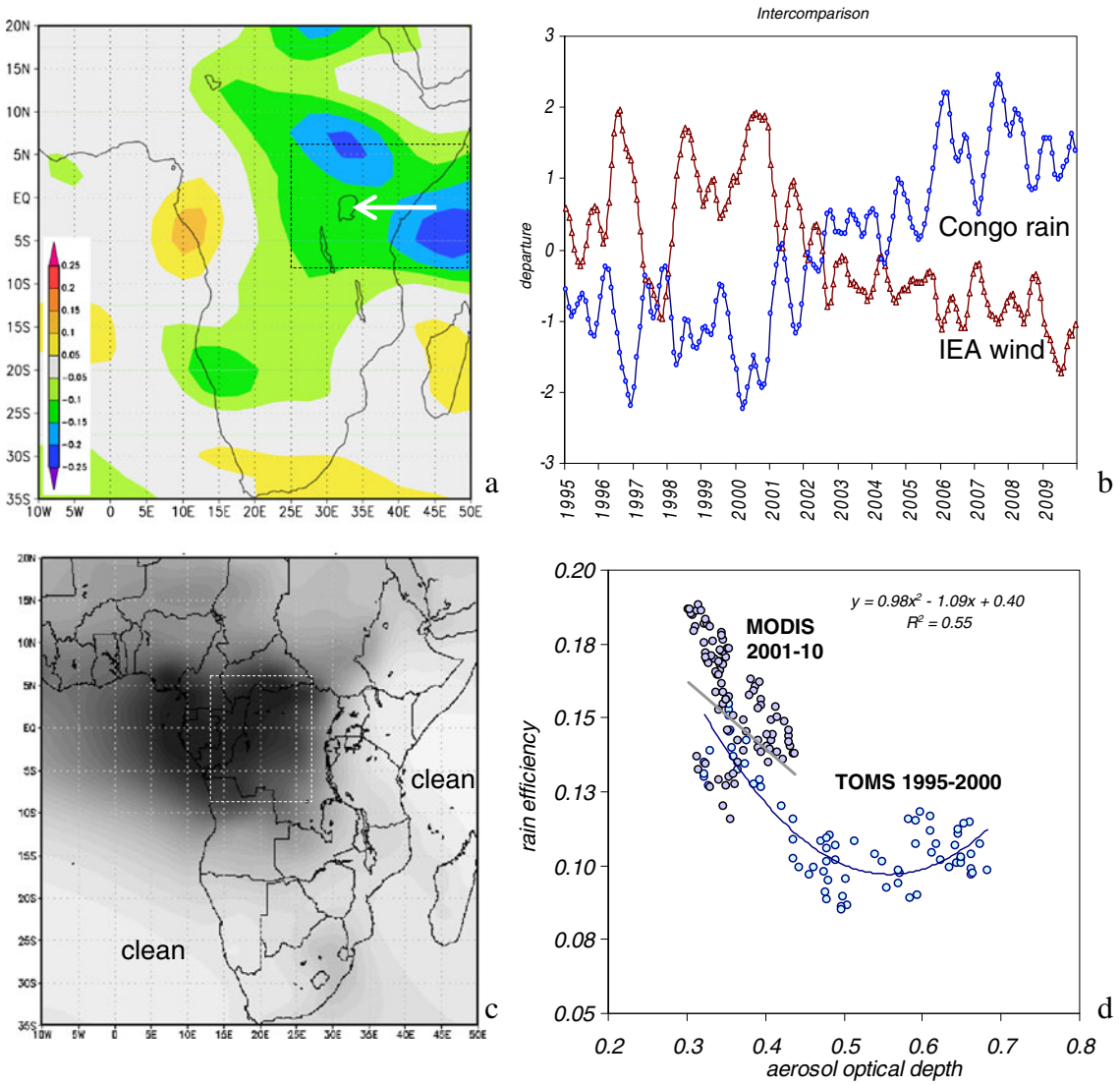

Fig. 7 **a** Linear regression trend of CFS 700-mb zonal winds, *blue* = easterly (in meters per second per year), and **b** time series of CFS IEA wind and CFS + ECMWF averaged Congo rain departures. **c** Climatology of MODIS aerosol optical depth (0–0.5 dark). **d** Scatterplot of smoothed monthly CFS rain efficiency (rain/PW) vs. satellite aerosol optical depth in the Congo. Index areas shown in **a**, **c**

The air masses surrounding Africa have distinct characteristics as indicated by MODIS AOD (Fig. 7c). There is a climatological maximum (>0.4) over the Gulf of Guinea and Congo Basin where aerosols from smoke and dust plumes accumulate. The zone of high AOD extends northwest into the Sahel (>0.3). To the south and east of Africa, the air is clean with AOD <0.1. Thus, when the IEA wind strengthened after 2001, cleaner air was advected toward central Africa enabling more efficient cloud development: IEA wind and Congo AOD r=+0.70. The Congo CFS rainfall divided by precipitable water (efficiency) is compared with satellite-observed AOD in Fig. 7d. During the TOMS era 1995–2000 with AOD >0.5, the average convective efficiency was 12 %, while in the MODIS era 2001–2010 with cleaner air (AOD<0.4), the efficiency rose to 18 %. Cloud liquid water in MERRA reanalysis shows significant increases from 1995 to 2010 in the 600- to 700-mb layer, where aerosol concentrations are typically high (Jury and

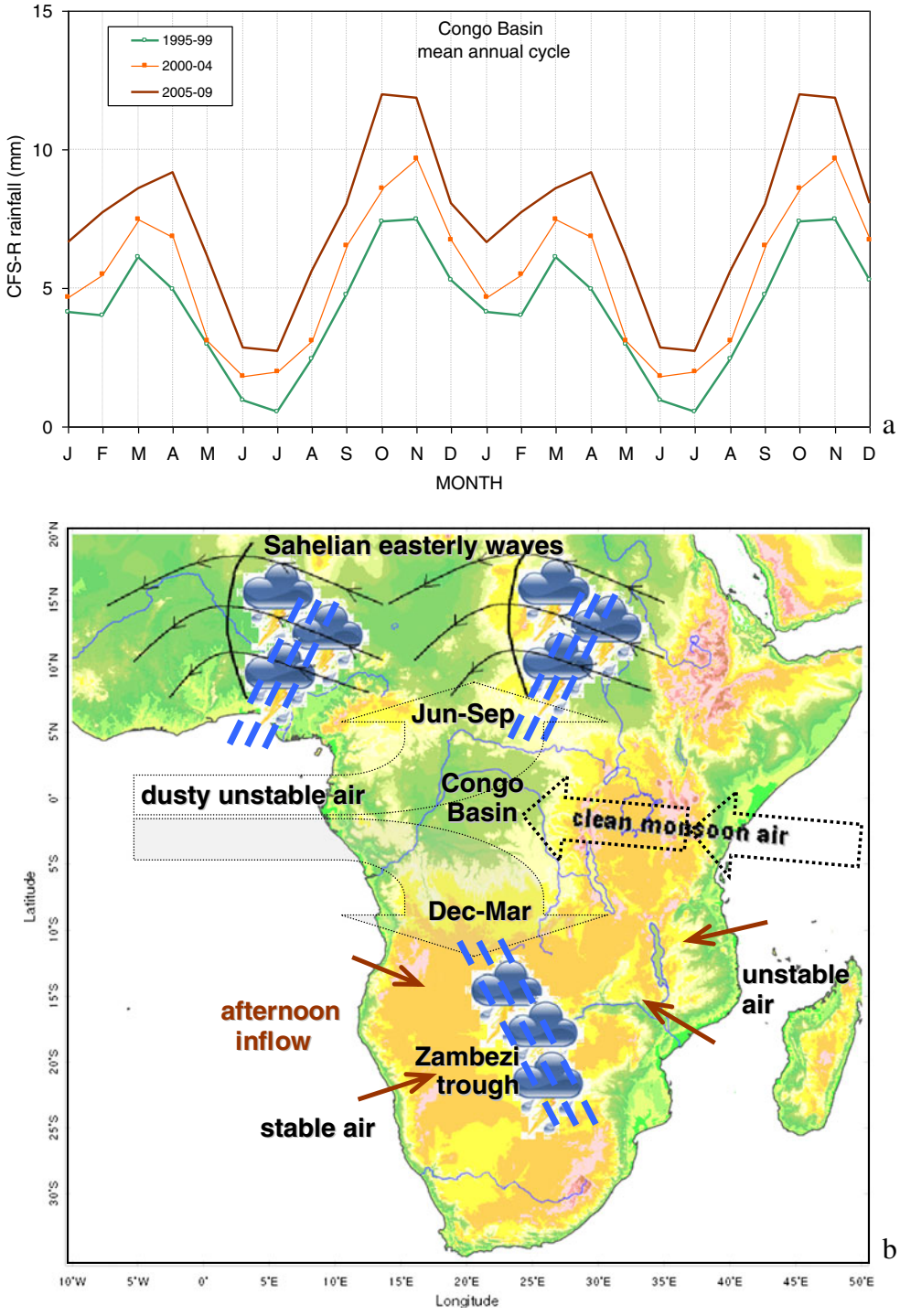

Fig. 8 **a** Mean annual cycle×2 of Congo rainfall in 5-year intervals. **b** Schematic of climate–weather interactions contributing to a return to wet conditions over Africa

Whitehall 2009). It is surmised that part of the flood trend over Africa is attributable to an influx of clean Indian Ocean air, together with a more effective scavenging of aerosols by the rain itself. Wetter conditions would also suppress dust and smoke plumes that are common to Africa.

A further question pertains to the seasonality of flood trend. For this, the mean annual cycle of monthly rainfall over the Congo Basin is analyzed (Fig. 8a). The increase of rainfall in the period 2005–2009 relative to the 1995–1999 period is evenly distributed, according to CFS data. Rainfall increases of 3.2 mm day^{-1} (σ=0.9) reach 4 mm day^{-1} in April, October, and November. Hence, additional convection is not focused in a particular season but spread over the year, possibly in relation to the aforementioned rising vegetation fraction (cf. Fig. 2e) that moistens the atmospheric boundary layer and generates persistence.

4 Discussion

Our ability to describe climatic trends over tropical Africa has matured with the advent of new datasets that offer confidence in data-sparse regions. Here, a return to wet conditions over Africa in the period 1995–2010 has been described using monthly river flow records, meteorological reanalysis data, and satellite observations. Up trends of rainfall anomalies over the Congo basin are evident; the ECMWF, CFS, GPCC average is +0.16 mm day^{-1} year^{-1}. Similarly, the river flow, runoff, and vegetation cover have risen over much of sub-Saharan Africa (except the east) and indicate that the climate has returned to wet conditions last seen in the 1950s (Hoerling et al. 2006). The wind patterns supporting the wet trend and flood events point to strengthened Hadley and Walker circulations that correspond with the tropical multi-decadal oscillation (Bell and Chelliah 2006). Increasing soil moisture and vegetation affect the atmospheric boundary layer, generating persistence.

The weather system responsible for Sahel floods includes more intense easterly waves, supported by a stronger temperature gradient north of the Congo. These have induced historical peaks of the Niger River (Amogu et al. 2010). The weather system driving Zambezi floods includes a tropical trough which draws moist equatorial air onto its eastern flank (Jury 2010a). An increasing land–sea temperature contrast accentuates onshore flow and uplift during the afternoon. The amplitude of diurnal rainfall increased threefold from 1995 to 2010 in the Zambezi Valley.

A key feature of the African flood trend is 700-mb zonal wind convergence from the equatorial Atlantic and Indian Oceans that is linked to the global climate system through mechanisms that are not yet fully understood. When SST in the central and east Atlantic warms during a combined NAO–AMO+ phase, there is a corresponding tropical circulation anomaly (Enfield and Mestas-Nunez 1999; Bell and Chelliah 2006) that results in low-level westerlies over the Gulf of Guinea. But the flood trend here is more closely tied to easterly winds over East Africa (cf. Fig. 7b), for which teleconnections are unclear. The aforementioned statistical correspondence with the AMO can be attributed to its slow rise to high phase over the 16-year period of study. Nonetheless, greater inflow to central Africa enhances vorticity and moisture available to easterly waves transiting the Sahel from June to September. During December to March season, when the ITCZ extends southward, equatorial moisture fluxes enrich Zambezi cloud bands. These features are schematically illustrated in Fig. 8b.

As tropical easterlies strengthened after 2001 in conjunction with coastal $\partial T/\partial x$, cleaner air was drawn from the Indian Ocean toward central Africa. Convective efficiency increased from an average of 12 % before 2001 to 18 % in 2006–2009 (cf. Fig. 7d). The increased rainfall suppressed dust and smoke plumes and scavenged aerosols. The return to wet conditions over Africa can be attributed to deep convection over the Congo that is redistributed to the subtropics through lateral coupling via Sahelian easterly waves and Zambezi troughs (Fig. 8b). This coupling may diminish if IPCC model projections are fulfilled (Meehl et al. 2007). Further efforts to better understand and predict climate–weather interactions will involve reestablishing observations in central Africa, applying cloud-resolving numerical models, and verifying responses using satellite-observed water levels.

Acknowledgments The author thanks the suppliers of data: Niger Basin Authority, Zambezi River Authority, KNMI Climate Explorer, IRI Climate Library, and NASA-Giovanni.

References

Amogu O, Descroix L, Yéro KS, Le Breton E, Mamadou I, Ali A, Vischel T, Bader J-C, Moussa IB, Gautier E, Boubkraoui S, Belleudy P (2010) Increasing river flows in the Sahel? Water 2:170–199

Anderson J, Hoar T, Raeder K, Liu H, Collins N, Torn R, Avellano A (2009) The data assimilation research testbed: a community facility. Bull Am Meteorol Soc 90:1283–1296

Bell GD, Chelliah M (2006) Leading tropical modes associated with interannual and multidecadal fluctuations in North Atlantic hurricane activity. J Climate 19:590–612

Bengtsson L et al (2007) The need for a dynamical climate reanalysis. Bull Am Meteorol Soc 88:495–501

Blunden J, Arndt DS, Baringer MO (2011) State of the climate in 2010. Bull Am Meteorol Soc 92:266

Bosilovich M (2008) NASA's modern era retrospective analysis for research and applications: integrating Earth observations. Earthzine

Camberlin P, Janicot S, Poccard I (2001) Seasonality and atmospheric dynamics of the teleconnection between African rainfall and tropical sea surface temperature: Atlantic vs. ENSO. Int J Climatol 21:973–1005

Chen Y, delGenio AD (2008) Evaluation of tropical cloud regimes in observations and a general circulation model. Clim Dyn. doi:10.1007/s00382-008-0386-6

Compo GP, Whitaker JS, Sardeshmukh PD (2006) Feasibility of a 100-year reanalysis using only surface pressure data. Bull Am Meteorol Soc 87:175–190

Compo GP et al (2011) The twentieth century reanalysis project. Quarterly J Roy Meteorol Soc 137:1–28

Conway D, Persechino A, Ardoin-Bardin S, Hamandawana H, Dieulin C, Mahé G (2009) Rainfall and water resources variability in sub-Saharan Africa during the twentieth century. J Hydrometeorol 10:41–59

Dee DP et al (2011) The ERA-Interim reanalysis: configuration and performance of the data assimilation system. Quart J Royal Meteorol Soc 137:553–597

Dinku T, Connor SJ, Ceccato P, Ropelewski CF (2008) Comparison of global gridded precipitation products over a mountainous region of Africa. Int J Climatol 28:1627–1638

Ek MB, Mitchell KE, Lin Y, Rogers E, Grunmann P, Koren V, Gayno G, Tarplay JD (2003) Implementation of Noah land surface model advances in the National Centers for Environmental Prediction operational mesoscale Eta model. J Geophys Res 108:8851. doi:10.1029/2002JD003296

Enfield DB, Mestas-Nuñez AM (1999) Multiscale variabilities in global sea surface temperatures and their relationships with tropospheric climate patterns. J Climate 12:2719–2733

Geerts B, Dejene T (2005) Regional and diurnal variability of the vertical structure of precipitation systems in Africa based on spaceborne radar data. J Climate 18:893–916

Hastenrath S, Polzin D, Mutai C (2011) Circulation mechanisms of Kenya rainfall anomalies. J Climate 24:404–412

Hirst AC, Hastenrath S (1983) Diagnostics of hydrometeorological anomalies in the Congo basin. Q J R Meteorol Soc 109:881–892

Hoerling M, Hurrell J, Eischeid J, Phillips A (2006) Detection and attribution of twentieth-century northern and southern African rainfall change. J Climate 19:3989–4008

Hong S-Y, Pan H-L (1996) Nonlocal boundary layer vertical diffusion in a medium-range forecast model. Mon Weather Rev 124:2322–2339

Jury MR (2003) Coherent variability of African River flows, composite climate structure and the Atlantic circulation. Water SA 29:1–10

Jury MR (2010a) Flood-producing cloud bands over the Kalahari Desert. Theor Appl Climatol 102:367–378

Jury MR (2010b) Meteorological scenario of Ethiopian floods in 2006–07. Theor Appl Climatol 104:209–219

Jury MR, Whitehall K (2009) Warming of an elevated layer over Africa. Clim Chang. doi:10.1007/s10584-009-9657-4

Jury MR, Matari EE, Matitu M (2008) Equatorial African climate teleconnections. Theor Appl Climatol 95:407–416

Kanamitsu M, Ebisuzaki W, Woollen J, Yang SK, Hnilo JJ, Fiorino M, Potter GL (2002) NCEP–DOE AMIP-II Reanalysis (R-2). Bull Am Meteorol Soc 83:1631–1643

Leptoukh G, Csiszar I, Romanov P, Shen S, Loboda T, Gerasimov I (2007) NASA NEESPI data and services center for satellite remote sensing information. Environ Res Lett 2:1748–1754

Love TB, Kumar V, Xie P and Thiaw W (2004) A 20-year daily Africa precipitation climatology using satellite and gauge data. Proc. 84th AMS Annual Meeting, Conf. Appl Climatol P5.4, Seattle

McCollum JR, Gruber RA, Ba MB (2000) Discrepancy between gauge and satellite estimates of rainfall over equatorial Africa. J Appl Meteorol 39:666–679

Meehl GA, Covey C, Taylor KE, Delworth T, Stouffer RJ, Latif M, McAvaney B, Mitchell JFB (2007) The WCRP CMIP3 multi-model dataset: a new era in climate change research. Bull Am Meteorol Soc 88:1383–1394

Mesinger F et al (2006) The North American regional reanalysis. Bull Am Meteorol Soc 87:343–360

Mutai CC, Ward NM (2000) East African rainfall and the tropical circulation/convection on intraseasonal to interannual timescales. J Climate 13:3915–3939

Olsson L, Eklundh L, Ardö J (2005) A recent greening of the Sahel: trend, patterns and potential causes. J Arid Environ 63:556–566

Pan H-L, Wu W-S (1995) Implementing a mass flux convective parameterization package for the NMC Medium-Range Forecast model. NMC Office Note 409, p. 40

Reason CJC, Landman W, Tennant W (2006) Seasonal to decadal prediction of southern African climate and its links with variability of the Atlantic Ocean. Bull Am Meteorol Soc 87:941–955

Rienecker MM et al (2011) MERRA: NASA's modern-era retrospective analysis for research and applications. J Climate 24:3624–3648

Rudolf B, Becker A, Schneider U, Meyer-Christoffer A, Ziese M (2010) The new GPCC Full Data Reanalysis Version 5, providing high-quality gridded monthly precipitation data for the global land-surface. Global Precipitation Climatology Centre, Technical Report (gpcc.dwd.de)

Saha S et al (2010) The NCEP climate forecast system reanalysis. Bull Am Meteorol Soc 91:1015–1057

Smith TM, Reynolds RW, Peterson TC, Lawrimore J (2008) Improvements to NOAA's historical merged land-ocean surface temperature analysis (1880–2006). J Climate 21:2283–2296

Tazalika L, Jury MR (2008) Spatial and temporal patterns of intra-seasonal rainfall oscillations over tropical Africa: their evolution and propagation. Theor Appl Climatol. doi:10.1007/s00704-007-0349-6

Todd MC, Washington R (2004) Climate variability in central equatorial Africa: influence from the Atlantic sector. Geophys Res Lett 31:23201–23205

Vorosmarty CJ, Fekete BM, Tucker BA (1998) Global River Discharge (v2) Data set. Oak Ridge National Laboratory Distributed Archive, Tennessee

Ward MN (1998) Diagnosis and short-lead time prediction of summertime rainfall in tropical North Africa at interannual and multidecadal timescales. J Climate 11:3167–3191

Zipser EJ (2003) Some views on hot towers after 50 years of tropical field programs and 2 years of TRMM data. In: Tao W-K, Adler R (eds) Cloud systems, hurricanes and TRMM. Monograph 51, Amer. Meteorol. Soc. Boston, pp. 49–58